

# Threshold Voltage Extraction Method for 2D Devices with Power-law $\mu(n_s)$ Dependence

Vincent Mosser, David Seron, and Youcef Haddab

Itron France, Issy Technology Center, 52 rue Camille Desmoulins, F-92448 Issy-les-Moulineaux, France  
vincent.mosser@itron.com, +33 1 4662 2429

**Keywords: FET, Threshold Voltage, Mobility, Power-law Dependence**

## Abstract

A new method for the extraction of the threshold voltage in Field-Effect-Transistors is presented. It is suited for all classes of devices whose mobility exhibits a power-law dependence on carrier concentration. The extracted threshold voltage  $V_T$  has a physical meaning: the sheet carrier concentration is proportional to  $V_G - V_T$ , as was shown using Hall studies in companion gated Hall devices.

## INTRODUCTION

Threshold voltage is with transconductance one of the most fundamental parameters characterizing a Field-Effect-Transistor (FET). It roughly corresponds to the gate voltage above which the drain-source current  $I_{DS}$  becomes appreciable and the  $I_{DS}(V_G)$  characteristics becomes more or less linear. However, due in particular to the fact that the constraints for various needs such as modeling, technology characterization or production assessment are not the same, there is no generally accepted unique definition of  $V_T$ .

Among the profusion of definitions used in the literature [1], many are phenomenological: the "threshold voltage" may correspond to the gate voltage for a given small  $I_{DS}$  current value, or be the intercept at  $I_{DS}=0$  of the extrapolation of a linear region in the  $I_{DS}(V_G)$  characteristics, or of the transconductance  $g_m(V_G)$  characteristics, etc...

A more physical method is the ratio method [2-5], based on the assumption that the inverse mobility has a linear variation as a function of the carrier channel density  $n_s = n_0 \times (1 + (V_G - V_T)/V_0)$ . Based on this assumption, it can

be shown that the ratio  $I_{DS} / \sqrt{g_m}$  (sometimes termed the Y-function) should be proportional to  $V_G - V_T$ , and should not depend on the mobility variation parameter [2], nor on the drain and source series access resistance [3].

However, this procedure doesn't provide reliable results when the assumption on the mobility fails. This is notably the case for a variety of devices and technologies, for which the mobility dependence on the channel sheet carrier concentration is fairly well described using a power-law behavior:  $\mu \propto n_s^\alpha$ . In compound semiconductor devices, this was observed e.g. in low density GaN/AlGaN/GaN heterostructures [6] or high-mobility InSb/InAlSb heterostructures [7]. Fig.1 shows the mobility behavior

$\mu \propto n_s^{0.74}$  measured in Hall devices made using AlGaAs/GaNAs/GaAs pseudomorphic structures. Moreover, this

behavior is also common in non-III-V devices, such as polycrystalline silicon based Thin-Film-Transistors (TFT) [8], or organic transistors such as oligothiophene TFT [9].

We propose a new simple and robust method for the determination of the threshold voltage in FETs with power-law  $\mu \propto n_s^\alpha$  dependence valid in some range above threshold. The resulting threshold value is independent of parasitic series resistances such as the drain and source access resistance, and of course of the mobility variation.

This physically based method is illustrated using experimental results from pHEMT transistors. The threshold voltage  $V_T$  extracted from these measurements compares well with the value obtained from the dependence of the sheet electron density  $n_s(V_G) \propto (V_G - V_T)$ , that is measured through Hall measurements in pHEMT like gated Hall devices fabricated in the same wafers.

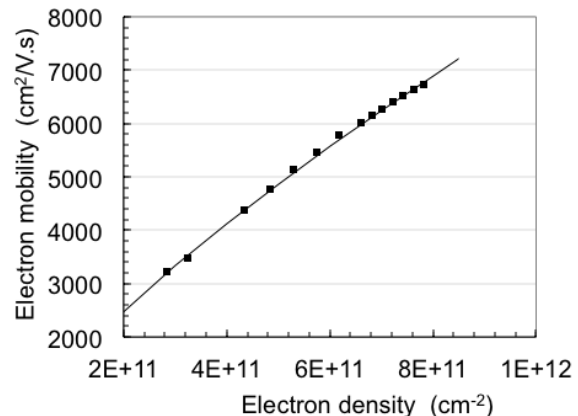


Fig.1 Mobility dependence on the channel electron density measured using a Hall cross shaped AlGaAs/InGaAs/GaAs pHEMT with a gate all over the channel (see Fig.3). The mobility shows a power-law dependence on the electron density, with exponent determined to be  $\alpha=0.74$ .

## THRESHOLD VOLTAGE EXTRACTION

In III-V based FETs, there is a small ungated region in series with the gated channel between the source and drain contacts, as shown in the schematic view of a heterostructure based FET in Fig.2. Using a standard approach derived from the archetypal long-channel MOSFET 1D approximation [10], it can be shown that, at least for low drain-source bias when the channel electrons are in the mobility regime,

the drain-source current is related to the channel potential at points  $y_1$  and  $y_2$  (Fig.2) through:

$$I_{DS} = \frac{W}{L_G} \times n_s \times C_0 \times V_G - V_T \frac{V_1 + V_2}{2} \times V_2 - V_1 \quad (1)$$

In (1),  $C_0$  is essentially the gate-channel specific capacitance,  $L_G = y_2 - y_1$  is the gate length,  $W$  is the channel width, and  $V_1 = V(y_1)$  and  $V_2 = V(y_2)$  are respectively the channel potential at the abscissae  $y_1$  and  $y_2$  in the channel (Fig.2).

Denoting  $V_S$  and  $V_D$  the potentials imposed externally to the source and drain contacts, one has:

$$V_1 = V_S + R_{acc} I_{DS} \quad \text{and} \quad V_2 = V_D - R_{acc} I_{DS}, \quad (2)$$

where the access resistance  $R_{acc}$  is the sum of the drain or source ohmic contact resistance in series with the resistance of the associated ungated portion of the channel. Inserting (2) in (1), one gets after trivial manipulation

$$I_{DS} = \frac{\frac{W}{L_G} \times n_s \times C_0 \times V_G - V_T \frac{V_{DS}}{2}}{1 + 2R_{acc} \times \frac{W}{L_G} \times n_s \times C_0 \times V_G - V_T \frac{V_{DS}}{2}}, \quad (3)$$

which is identical to the general expression of the drain-source current  $I_{DS}$  in a silicon MOSFET when the access resistances are taken into account [3]. The electron density  $n_s(y)$  is very slightly modulated due to the voltage drop along the channel, its mean value is related to the gate and drain bias through:

$$n_s = \frac{C_0}{e} (V_G - V_T - V_{DS}/2). \quad (4)$$

The mobility dependence on  $n_s$ , or equivalently on  $V_G$ ,

$$\mu_n = \mu_{n0} \times \frac{n_s}{n_{s0}} \quad \text{or} \quad \mu_n = \mu_{n0} \frac{(V_G - V_T - V_{DS}/2)}{(V_{G0} - V_T - V_{DS}/2)} \quad (5)$$

valid for any arbitrary  $(\mu_{n0}, n_{s0})$  conditions, is injected in (3) before calculating the total channel resistance  $R = V_{DS}/I_{DS}$ :

$$R = 2R_{acc} + K (V_G - V_T - V_{DS}/2)^{(1+)} \quad (6)$$

where the coefficient  $K$  stands for the expression:

$$K = \frac{L_G}{W} \times \frac{1}{n_{s0} \times C_0} (V_{G0} - L_G - L_G/2). \quad (7)$$

The first derivative wrt.  $V_G$  of the channel resistance reads:

$$R' = -\frac{dR}{dV_G} = (1+ ) K (V_G - V_T - V_{DS}/2)^{(2+)} \quad (8)$$

and its 2<sup>nd</sup> derivative is:

$$R'' = \frac{d^2 R}{dV_G^2} = (1+ )(2+ ) K (V_G - V_T - V_{DS}/2)^{(3+)} \quad (9)$$

Finally, it turns out that the ratio  $-R'/R''$  is expected to depend on  $V_G$  in a linear way, without any dependence on the various device parameters introduced in (3):

$$\frac{R'}{R''} = \frac{1}{2+} \times V_G - V_T - \frac{V_{DS}}{2} \quad (10)$$

Thus, the  $-R'/R''$  against  $V_G$  graph should be a straight line intercepting the x-axis at  $V_T - V_{DS}/2$ , and whose slope is

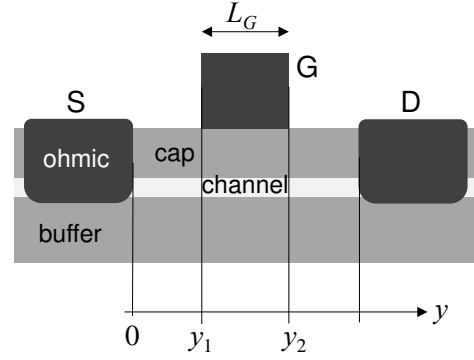


Fig.2 Schematic view of the cross-section of a heterostructure based FET, with definition of the points  $y_1$  and  $y_2$  along the channel.

directly related to  $\alpha$ , the exponent in the mobility expression.

The  $-R'/R''$  ratio vs.  $V_G$  can be easily computed from a discrete  $I_{DS}(V_G)$  characteristics taken at equally spaced points  $V_{G_n}$  with  $V_{G_{n+1}} - V_{G_n} = V_G$ . From the Taylor expansion:

$$R_{n\pm 1} \approx R_n \pm R'_n V_G + R''_n V_G^2/2 \quad (11)$$

the ratio can be computed as:

$$\left. \frac{R'}{R''} \right|_n = \frac{(R_{n-1} - R_{n+1})}{R_{n+1} - 2R_n + R_{n-1}} \cdot \frac{V_G}{2}. \quad (12)$$

In the subthreshold region, the free carrier density depends exponentially on  $V_G$ , and hence the subthreshold drain-source current reads:

$$I_{DS} \mu \exp \frac{V_G - V_T}{kT} \quad (13)$$

where  $\lambda$  denotes some capacitance ratio [11], larger than 1 depending on the kind of FET. With the same definitions as before, one can easily check that:

$$R_{n\pm 1} = \exp(\mp \frac{\Delta V_G}{\lambda kT}) R_n, \quad (14)$$

and the value of  $-R'/R''$  computed according to (12) reads:

$$\left. \frac{R'}{R''} \right|_n = \frac{V_G}{2} \cdot \coth \frac{V_G}{2 kT} \quad (15)$$

The  $-R'/R''$  plot tends towards a constant for  $V_G < V_T$ , which is approximately equal to  $V_G/2$  as soon as  $V_G > 2 kT$ .

## EXPERIMENTAL

The devices used in this study are based on AlGaAs/InGaAs/GaAs pseudomorphic heterostructures on a semi-insulating substrate, designed for the manufacturing of high-sensitivity Hall effect devices with excellent metrological performances [12]. Wafers were grown by various providers, using MBE. The QW channel mainly consists of a 10 or 13 nm thick  $\text{In}_y\text{Ga}_{1-y}\text{As}$  layer with In content  $y$  amounting to 15% or 20%, depending on the wafers. Free electrons in the channel are provided by a delta doping layer in the  $x \approx 30\%$   $\text{Al}_x\text{Ga}_{1-x}\text{As}$  cap layer. Doping

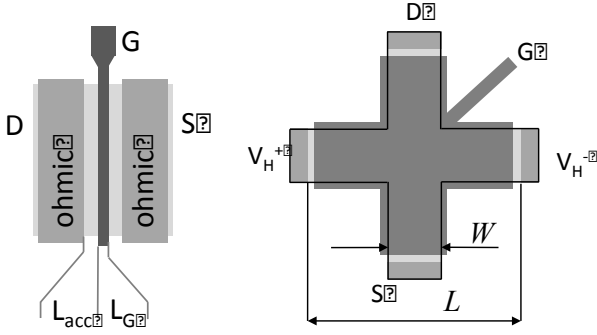


Fig.3. Schematic view of the devices used in this study. Left: normally-on FET, with access length  $L_{acc}$  on each side of the gated region and gate length  $L_G$ . Right: Gated Hall device. Channel length  $L=200\ \mu\text{m}$ , arm width  $W=50\ \mu\text{m}$ .

density was chosen to get an  $n_s=6.5$  to  $9 \times 10^{11}\text{cm}^{-2}$  electron density. The cap layer  $L_A$  is rather thick, between 100 nm and 260 nm, depending on the wafers. In this case, the gate-channel capacitance is essentially due the cap layer thickness  $C_0 \approx \epsilon_s/L_A$ , with low influence of the capacitance due to the finite 2D density-of-states in the quantum well, or from other quantum effects.

From these wafers, two kinds of devices were fabricated. For the transistor studies, several series of normally-on pHEMT as depicted in Fig.3 were designed using optical lithography. The gate length  $L_G$  was varied between 1 and 15  $\mu\text{m}$ . The ungated access length  $L_{acc}$  between each drain or source region and the gated portion of the channel was varied between 1.5 and 3  $\mu\text{m}$ . The channel width is comprised between 10 and 100  $\mu\text{m}$ . Typical  $I_{DS}(V_G)$  results are shown in Fig.4.

For the Hall effect measurements, Greek-cross shaped Hall effect devices were designed (Fig.3), with a gate covering almost the entire active region between contacts. Thus, the electron density remains homogenous when varying the gate voltage, at least as long as the ohmic voltage drop in the sample, remains small.

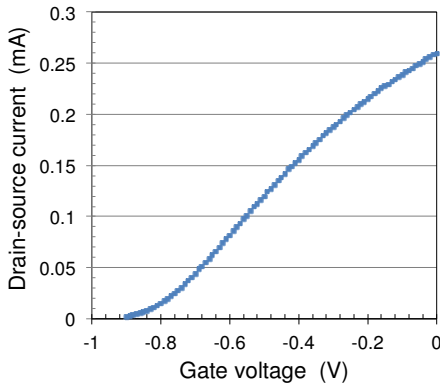


Fig.4  $I_{DS}(V_G)$  characteristics of a jumbo pHEMT transistor with 2  $\mu\text{m}$  gate length and 2  $\mu\text{m}$  access length between ohmic contact and gate. Cap layer thickness is about 110 nm.

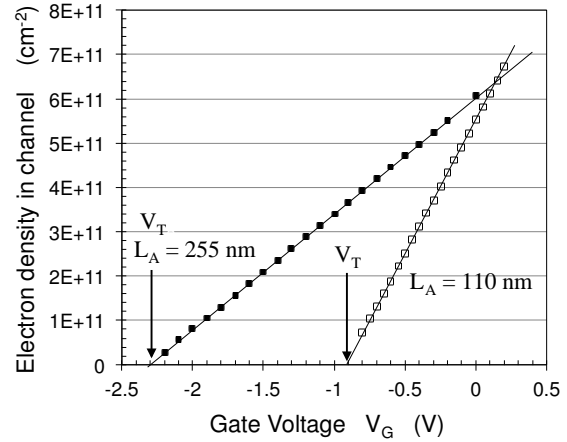


Fig.5 Experimental dependence of the Hall electron density in Hall cross-shaped AlGaAs/InGaAs/GaAs pHEMT-like Hall devices with cap layer thickness 110 and 255 nm. The electron density increases proportionally with the  $V_G$  increase, unambiguously defining a threshold voltage  $V_T$ .

In order to remain within Van der Pauw conditions [13], and thus to allow for precise Hall measurements, we took several precautions. The complete gate covering ensures that the electron density remains homogenous for every gate voltage value. The Greek crosses have a  $L/W=4$  geometry in order to avoid shunting by the lateral electrodes. Indeed, under such conditions, the geometrical factor  $G_H$  in the Hall voltage [13] is practically equal to unity [14]. Finally, the  $V_H(V_G)$  characteristics were measured using a constant low bias voltage  $V_{in}$  equal to 20 mV, the bias current  $I_{in}$  was measured and used in (16) to calculate  $n_s$ .

Moreover, in a degenerate QW Hall, the scattering factor  $r_H$  can be assumed to be unity too.

Thus, measuring the Hall voltage:

$$V_H = \frac{G_H \kappa_H}{en_s} I_{in} B = \frac{1}{en_s} I_{in} B \quad (16)$$

allows for an accurate determination of the sheet carrier density as a function of  $V_G$ . Combining it with sheet resistivity  $R_{sq}(V_G)$  obtained from standard Van der Pauw resistivity measurements as a function of the gate voltage yields

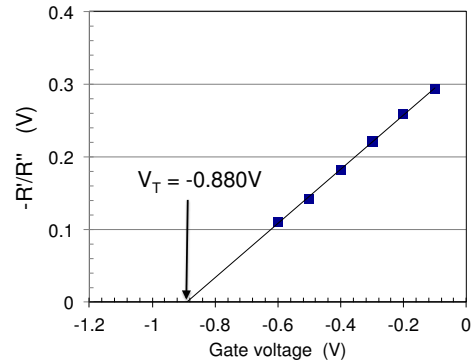


Fig.6 Ratio  $-R'/R''$  calculated by applying Eq.(12) to the  $I_{DS}(V_G)$  data of Fig.4, for  $\Delta V_G=100\ \text{mV}$ . The ratio shows a linear dependence on  $V_G-V_T$ . The threshold voltage is very close to that determined by Hall measurements in Hall devices from the same wafer.

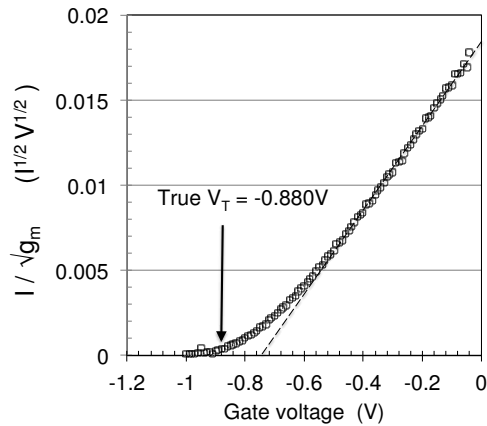


Fig.7 Standard  $I_{DS}/\sqrt{g_m}$  ratio method applied to the  $I_{DS}(V_G)$  data of Fig.4. The curvature of the curve renders the extraction of a threshold voltage more difficult. The intercept of the dashed curve is more than 150mV apart from the true threshold voltage.

the mobility dependence  $\mu_n(V_G)$  or  $\mu_n(n_S)$  shown in Fig.1. The linear behavior of  $n_S(V_G)$  is shown in Fig.5 for two devices with cap layer thickness 100nm and 260 nm.

#### THRESHOLD VOLTAGE EXTRACTION – DISCUSSION

The quantity  $-R'/R''$  obtained using Eq.(12) from the  $I_{DS}(V_G)$  data of Fig.4. is perfectly linear (Fig.6). The determined  $V_T = -880$  mV fits closely with the Hall  $n_S(V_G)$  value, -900 mV. Note that the devices were 6 mm from each other. On the contrary, the standard  $I_{DS}/\sqrt{g_m}$  ratio method lacks linearity and yields a value different by more than 150 mV (Fig.7). Fig.8 shows the robustness of the method. The  $V_T$  values obtained by choosing 3 different  $V_G$  increments of 0.2, 0.4 and 0.6 V perfectly coincide. The asymptotes at  $V_G/2$  for  $V_G < V_T$  are in agreement with Eq.(15). Fig.8 also suggests that just a few widely spaced  $I_{DS}(V_G)$  points above threshold are sufficient to get a precise determination of  $V_T$ , thus limiting the effect of noise in the procedure.

#### CONCLUSION

A new physical model, valid in the case of mobility with power-law dependence on the sheet carrier density, has been proposed for the extraction of the threshold voltage in FETs. It relies on the calculation of the  $-R'/R''$  quantity from a few  $I_{DS}(V_G)$  data above threshold. The result is independent of the mobility variation and series resistance. This model has been tested and validated up to now for AlGaAs/InGaAs/GaAs devices with a rather thick cap layer ( $\approx 100$  nm). Owing to the fact that it provides a threshold voltage value with clear physical meaning, it would be interesting to check whether it also holds for other kinds of devices. When performing coupled field-effect transistor and Hall measurements, care should be taken to design Hall devices with negligible short-circuit current [11] in the lateral contacts.

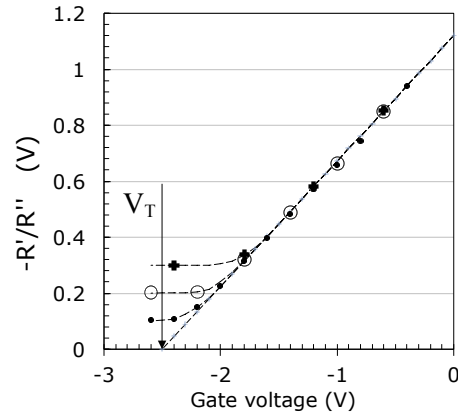


Fig.8 Ratio  $-R'/R''$  for a transistor with large cap layer (258 nm), calculated for different values of the  $V_G$  increment.  $\Delta V_G$  is respectively equal to 200 (small dots), 400 (large hollow dots) and 600 mV (thick crosses). The curves show a linear dependence on  $V_G - V_T$  for large enough  $V_G$ , and an asymptotic behavior  $-R'/R'' \rightarrow \Delta V_G/2$  below and around  $V_T$ .

#### ACKNOWLEDGEMENTS

This work was partly funded by grant No. ANR-07-Blan-0368 "Micromag". Thanks are due to Sh. Bansropun and the Thales Research&Technology clean room staff in Palaiseau for fabricating some of the devices used in this study.

#### REFERENCES

- [1] A. Ortiz-Conde, F.J. García Sánchez, J.J. Liou, A. Cerdeira, M. Estrada, Y. Yue, *Microelectronics Reliability* 42, 583–596 (2002)
- [2] G. Ghibaudo, *Electron. Lett.*, 24, 543-545 (1988)
- [3] S. Jain, *IEE Proc., Part I: Solid-State Electron Dev.* 135, 162-164 (1988)
- [4] W. Fikry, G. Ghibaudo, H. Haddara, S. Cristoloveanu, M. Dutoit, *Electron. Lett.* 31, No.2, 762-764 (1995)
- [5] P.K. McLarty, S. Cristoloveanu, O. Faynot, V. Misra, J.R. Hauser, J.J. Wortman, *Solid-State Electronics* 38, 1175-1177 (1995)
- [6] M.J. Manfra, K.W. Baldwin, A.M. Sergent, R.J. Molnar and J. Caissie, *Appl. Phys. Lett.* 85, 1722-1724 (2004)
- [7] A.M. Gilbertson, W.R. Branford, M. Fearn, L. Buckle, P.D. Buckle, T. Ashley, and L.F. Cohen, *Phys. Rev. B* 79, 235333 (2009)
- [8] Mark D. Jacunski, Michael S. Shur, and Michael Hack, *IEEE Trans. Electron Dev.* 43, 1433-1440 (1996)
- [9] G. Horowitz, M.E. Hajlaoui, and R. Hajlaoui, *J. Appl. Phys.* 87, 4456-4463 (2000)
- [10] S.M. Sze and K.K Ng, *Physics of semiconductor devices*, 3rd ed., John Wiley & Sons (2006).
- [11] R.J. van Overstraeten, G.J. Declerck, P.A. Muls, *IEEE Trans. Electron Dev.*, 22, 282-288 (1975).
- [12] V. Mosser, A. Kerlain, Y. Haddab, R. Morton and M.J. Brophy, *Ensuring high yield and good reliability for mass-produced high-performance Hall effect sensors*, 2006 GaAs ManTech Technical Digest, Vancouver, BC, Canada, pp. 291-294, April 2006.
- [13] R.S. Popovic, "Hall Effect Devices", 2nd ed., IOP Publishing, Bristol and Philadelphia, 2004.
- [14] J. Przybytek, V. Mosser and Y. Haddab, *LF noise in cross Hall effect devices -geometrical study*, Proc. SPIE Vol. 5113, 475-483, May 2003

#### ACRONYMS

FET:	Field Effect Transistor
MBE:	Molecular Beam Epitaxy
pHEMT:	Pseudomorphic High Electron Mobility Transistor
QW:	Quantum Well